RESEARCH PAPER

Dynamics of cholera disease by using two recent fractional numerical methods

Pushpendra Kumar ⓘ[1,*,‡] and Vedat Suat Erturk ⓘ[2,‡]

[1]Department of Mathematics and Statistics, School of Basic and Applied Sciences, Central University of Punjab, Bathinda, Punjab-151001, India , [2]Department of Mathematics, Ondokuz Mayis University, Atakum-55200, Samsun, Turkey

*Corresponding Author
‡kumarsaraswatpk@gmail.com (Pushpendra Kumar); vserturk@omu.edu.tr (Vedat Suat Erturk)

Abstract

In this paper, we simulate an epidemic model of cholera disease in the sense of generalized Liouville-Caputo fractional derivative. We provide the results related to the existence of a unique solution by using some well-known theorems. Numerical solutions of the given model are derived by using two different numerical methods along with their importance. A number of graphs are plotted to understand the given cholera disease dynamics. The main motivation to do this research is to understand the given disease dynamics as well as the efficiency of both methods which are very recent to the literature.

Key words: Cholera disease; mathematical model; generalized Liouville-Caputo fractional derivative; numerical methods; graphical simulations
AMS 2020 Classification: 26A33; 34C60; 92C60; 92D30

1 Introduction

The bacterium 'Vibrio Cholerae' causes cholera, which is a bacterial illness. This bacterium is commonly found in contaminated foods. It's a Gram-negative bacteria which is curved and comma-shaped. It may be found in sewage and coastal saltwater environments. It's also found where there aren't enough sanitary facilities. During the 1800s, this illness was initially discovered in the United States. For hundreds of years, humans have been suffering from cholera sickness. If left untreated, this condition can cause severe diarrhoea and dehydration in the body. It can sometimes result in a deadly condition. They cling to shellfish, crabs, and other creatures' shells. Various illnesses, including cholera, are spread by drinking polluted water. This bacteria dwells in the human body's small intestine and releases an exotoxin, which induces a flow of water and electrolytes into the small intestine, including sodium bicarbonate, chloride, and others [1, 2].

Causes of cholera: (i) It is brought on by causes such as a polluted water source. (ii) It occurs as a result of the intake of tainted foods and beverages offered by street vendors. (iii) Vegetables that are cultivated with the help of human waste and water. (iv) Contaminated seafood, which has been contaminated by sewage. (v) Foods that have an adverse effect on the digestive system are to blame. Some of the symptoms of Cholera are: (i) High fever. (ii) Weight loss. (iii) Increased thirst. (iv) Feeling of Nausea. (v) Vomiting sensation. (vi) A kind bloating in the belly. (vii) Blood pressure becomes low. (viii) The elasticity of the skin is lost. (ix) Develop cramps in the muscles. (x) A rapid increase in the heart rate. (xi) Dryness in the mouth, nose, and eyelids. (xii) Formation of blood or mucus or sometimes undigested materials in the stool [1, 2].

Replacement of lost fluid and electrolytes is part of the cholera therapy. Dehydration may be avoided by drinking enough of ORS (Oral Rehydration Solution). Intravenous fluid replacement may be necessary if the disease worsens. Antibiotics and zinc supplements may be

prescribed by doctors to treat diarrhoea. Recently, some novel mathematical studies have been come out to define the dynamics of cholera. In [3], a cholera disease model with optimal control treatment is defined. Authors in ref. [4] have given some mathematical modelling related analysis on the dynamics of cholera. Study given in ref. [5] describes the transmission dynamics of cholera by using a mathematical modeling along with control strategies. In [6], spatial synchrony in fractional order metapopulation cholera transmission is given.

As we know that the fractional derivatives [7, 8] are helpful operators to study real-world problems in the sense of mathematical modeling. Recently, a number of studies have been coming to the literature on this topic. In the epidemic modelings, disease like COVID-19 [9, 10, 11, 12, 13, 14, 15, 16, 17, 18], cancer therapy [19], tuberculosis [20], malaria [21], lassa hemorrhagic fever [22], and canine distemper virus [23], etc. have been successfully studied. Applications of fractional derivatives in psychology [24], ecology [25, 26], and plant epidemiology [27, 28] have been derived by many researchers. Several novel fractional-order mathematical models for studying the calcium distribution in nerve cells are introduced in refs. [29, 30, 31, 32]. Also, some novel recent applications of fractional-order computational methods in different real-world problems can be studied from refs. [33, 34, 35, 36, 37]. Nowadays, scientists use different types of fractional derivatives with or without singular kernels in a huge amount to solve various types of real-world problems. In our study, we use the generalised Liouville-Caputo fractional derivative to simulate a mathematical model of the cholera epidemic. The novelty of this work is to explore the given disease dynamics as well as the efficiency of both numerical schemes which are very recent to the literature.

This article is divided into number of sections. After defining cholera epidemic, we mention two necessary definitions in Section 2. In Section 3, a cholera model followed by the fractional model is proposed. In Section 4, results related to existence and uniqueness analysis are given. The solution of the model by using two different numerical methods is given in Section 5. All results and discussion are explained in Section 6. Finally, concluding remarks are given in the last Section 7.

2 Preliminaries

Here we recall the definitions of two fractional derivatives.

Definition 1 *[8] The Liouville-Caputo non-integer order derivative of $\mathcal{L} \in C_{-1}^d$ is defined by*

$$D_t^\varrho \mathcal{L}(t) = \begin{cases} \frac{d^q \mathcal{L}(t)}{d\zeta^q}, & \varrho = q \in \mathbb{N} \\ \frac{1}{\Gamma(q-\varrho)} \int_0^t (t-\vartheta)^{q-\varrho-1} \mathcal{L}^{(q)}(\vartheta) \, d\vartheta, & q-1 < \varrho < q, q \in \mathbb{N}. \end{cases} \tag{1}$$

Definition 2 *[38] The generalized Liouville-Caputo-type non-integer order derivative, $D_{d_+}^{\varrho,\rho}$ of order $\varrho > 0$ is given by*

$$(D_{d_+}^{\varrho,\rho} \mathcal{L})(\xi) = \frac{\rho^{\varrho-q+1}}{\Gamma(q-\varrho)} \int_d^\xi s^{\rho-1} (\xi^\rho - s^\rho)^{q-\varrho-1} \left(s^{1-\rho} \frac{d}{ds} \right)^q \mathcal{L}(s) \, ds, \quad \xi > d, \tag{2}$$

where $\rho > 0, d \geq 0$, and $q - 1 < \varrho \leq q$.

3 Model description

Now we describe the dynamics of the mathematical model used to study the cholera epidemic. Recently, authors in ref. [4] proposed an integer-order mathematical model consisting following ordinary differential equations

$$\begin{cases} S' = b - dS - \beta SI + \nu V + \gamma R, \\ I' = -dI + \beta SI - \sigma I - \omega I - \alpha I, \\ R' = -dR + \alpha I - \gamma R, \\ V' = \sigma I - \nu V, \end{cases} \tag{3}$$

where $N = S + I + R + V$. In this model, the cholera disease is distributed into four classes. S is for susceptible class, I is for infected individuals at contact rate β, R is for recovered humans at a rate α and V is for the environment. A brief description of all parameter values is given in Table 1. The disease-free equilibrium is defined by

$$(S^*, 0, 0, 0) = \left(\frac{b}{d}, 0, 0, 0 \right). \tag{4}$$

The endemic equilibrium is

$$(S^{**}, I^{**}, R^{**}, V^{**}) = \left(\frac{(d+\omega+\sigma+\alpha)}{\beta}, \frac{(d+\gamma)R^*}{\alpha}, \frac{(d+\beta I^*)S^* - b}{\gamma}, \frac{\sigma(d+\gamma)R^*}{\nu\alpha} \right), \tag{5}$$

and then the basic reproductive number is calculated as

$$\mathcal{R}_0 = \frac{\beta b}{d} - (d+\omega+\sigma+\alpha). \tag{6}$$

Table 1. Parameter values cited from [4]

Parameter	Description	Values
b	Recruitment rate	0.000096274
d	Natural death rate	0.00002537
ω	Disease induced death rate	0.0004
α	Recovery rate	0.2
γ	Rate of recovered humans return to the susceptible class	0.002
σ	Rate of infectious humans contaminate the environment	0.1
ν	Environment infect humans with the bacteria at a rate	0.075
β	Contact rate with infectious humans	0.011

To capture the hysteresis memory effects in the given model, the generalization of the proposed model (3) in the generalised Liouville-Caputo sense is described as follows:

$$
\begin{cases}
{}^{C}D_t^{\varrho,\rho}S = b - dS - \beta SI + \nu V + \gamma R, \\
{}^{C}D_t^{\varrho,\rho}I = -dI + \beta SI - \sigma I - \omega I - \alpha I, \\
{}^{C}D_t^{\varrho,\rho}R = -dR + \alpha I - \gamma R, \\
{}^{C}D_t^{\varrho,\rho}V = \sigma I - \nu V.
\end{cases}
\tag{7}
$$

where ${}^{C}D_t^{\varrho,\rho}$ is the notation of generalised Caputo type fractional derivative operator with fractional order ϱ and the extra parameter ρ.

4 Existence and uniqueness analysis

In this section, we do the analysis for the existence of a unique solution to the proposed model with the help of the consequences of fixed point theory. We perform the analysis for class $S(t)$ and it is relevant to write that the same analysis will be applicable for the rest of the equations of model (7). Let us write the model (7) in the following compact form:

$$
\begin{cases}
{}^{C}D_t^{\varrho,\rho}S(t) = \mathcal{L}_1(t,S), \\
{}^{C}D_t^{\varrho,\rho}I(t) = \mathcal{L}_2(t,I), \\
{}^{C}D_t^{\varrho,\rho}R(t) = \mathcal{L}_3(t,R), \\
{}^{C}D_t^{\varrho,\rho}V(t) = \mathcal{L}_4(t,V),
\end{cases}
\tag{8}
$$

with the initial conditions $S(0) = S_0, I(0) = I_0, R(0) = R_0$, and $V(0) = V_0$.
For proving the analysis for $S(t)$ class, define the initial value problem (IVP)

$$
{}^{C}D_t^{\varrho,\rho}S(t) = \mathcal{L}_1(t,S),
\tag{9a}
$$

$$
S(0) = S_0.
\tag{9b}
$$

The relative Volterra integral equation of the above IVP is

$$
S(t) = S(0) + \frac{\rho^{1-\varrho}}{\Gamma(\varrho)} \int_0^t \theta^{\rho-1}(t^\rho - \theta^\rho)^{\varrho-1}\mathcal{L}_1(\theta,S)d\theta.
\tag{10}
$$

Now we proceed to the following results:

Theorem 1 *[39, 40] Let $0 < \varrho \leq 1$, $S_0 \in \mathbb{R}$, $K > 0$ and $T^* > 0$. Consider $\mathcal{L} := \{(t,S) : t \in [0,T^*], \ |S - S_0| \leq K\}$ and let the function $\mathcal{L}_1 : \mathcal{L} \to \mathbb{R}$ be continuous. Also, let $M := \sup_{(t,S)\in\mathcal{L}} |\mathcal{L}_1(t,S)|$ and*

$$
T = \begin{cases}
T^*, & \text{if} \quad M = 0, \\
min\{T^*, \left(\dfrac{K\Gamma(\varrho+1)\rho^\varrho}{M}\right)^{\frac{1}{\varrho}}\} & \text{otherwise.}
\end{cases}
\tag{11}
$$

Then, there exists a function $S \in C[0,T]$ that satisfies the IVP (9a) and (9b).

Theorem 2 *[39, 40] Let $S(0) \in \mathbb{R}$, $K > 0$, $T^* > 0$, $0 < \varrho \leq 1$. Define the set $\mathcal{L}$ as in Theorem 1 and let the function $\mathcal{L}_1 : \mathcal{L} \to \mathbb{R}$ be continuous and satisfies a Lipschitz condition with respect to the second variable, i.e.*

$$
|\mathcal{L}_1(t,S_1) - \mathcal{L}_1(t,S_2)| \leq L|S_1 - S_2|,
$$

for some constants $L > 0$ independent to t, S_1, and S_2. Then, there exists a unique solution $S \in C[0,T]$ for the IVP (9a) and (9b).

5 Numerical solution of the model

Solution of the projected model using modified Predictor–Corrector algorithm

Nowadays, a number of numerical methods are available in the literature. Recently, a modified version of the Predictor-Corrector (P–C) scheme to solve delay-type fractional initial value problems has been proposed in ref. [41]. In this part of the study, we write the numerical solution of the proposed cholera model with the help of the generalised P-C method investigated in ref. [38]. The reason to use this generalised Liouville-Caputo derivative is its features to generate more varieties in the graphical observations in the presence of both parameters ϱ and ρ. Now first we consider the solution for the first equation of the cholera model (7) by taking equivalent Volterra integral equation

$$S(t) = S(0) + \frac{\rho^{1-\varrho}}{\Gamma(\varrho)} \int_0^t \theta^{\rho-1} (t^\rho - \theta^\rho)^{\varrho-1} \mathcal{L}_1(\theta, S) d\theta. \tag{12}$$

Now by dividing the interval $[0, T]$ into N unequal sub-intervals $\{[t_k, t_{k+1}], \; k = 0, 1, ..., N - 1\}$ taking the mesh points

$$\begin{cases} t_0 = 0, \\ t_{k+1} = (t_k^\rho + h)^{1/\rho}, \quad k = 0, 1, ..., N - 1, \end{cases} \tag{13}$$

where $h = \dfrac{T^\rho}{N}$. Now, to evolute the approximations S_k, $k = 0, 1, ..., N$, we are assuming that we have already derived the approximations $S_j \approx S(t_j)(j = 1, 2, ..., k)$, and we want to calculate the approximation $S_{k+1} \approx S(t_{k+1})$ by means of the integral equation

$$S(t_{k+1}) = S(0) + \frac{\rho^{1-\varrho}}{\Gamma(\varrho)} \int_0^{t_{k+1}} \theta^{\rho-1} (t_{k+1}^\rho - \theta^\rho)^{\varrho-1} \mathcal{L}_1(\theta, S) d\theta. \tag{14}$$

Let us take $z = \theta^\rho$, we get

$$S(t_{k+1}) = S(0) + \frac{\rho^{-\varrho}}{\Gamma(\varrho)} \int_0^{t_{k+1}^\rho} (t_{k+1}^\rho - z)^{\varrho-1} \mathcal{L}_1(z^{1/\rho}, S(z^{1/\rho})) dz. \tag{15}$$

That is

$$S(t_{k+1}) = S(0) + \frac{\rho^{-\varrho}}{\Gamma(\varrho)} \sum_{j=0}^k \int_{t_j^\rho}^{t_{k+1}^\rho} (t_{k+1}^\rho - z)^{\varrho-1} \mathcal{L}_1(z^{1/\rho}, S(z^{1/\rho})) dz. \tag{16}$$

To approximate the right-hand side of Eq. (16), we use the trapezoidal quadrature rule with respect to the weight function $(t_{k+1}^\rho - z)^{\varrho-1}$, by replacing the function $\mathcal{L}_1(z^{1/\rho}, S(z^{1/\rho}))$ by its piecewise linear interpolant with nodes chosen at the t_j^ρ ($j = 0, 1, ..., k + 1$), then we obtain

$$\begin{aligned} \int_{t_j^\rho}^{t_{k+1}^\rho} (t_{k+1}^\rho - z)^{\varrho-1} \mathcal{L}_1(z^{1/\rho}, S(z^{1/\rho})) dz &\approx \frac{h^\varrho}{\varrho(\varrho+1)} \left[\left((k-j)^{\varrho+1} - (k-j-\varrho)(k-j+1)^\varrho \right) \mathcal{L}_1(t_j, S(t_j)) \right. \\ &\left. + \left((k-j+1)^{\varrho+1} - (k-j+\varrho+1)(k-j)^\varrho \right) \mathcal{L}_1(t_{j+1}, S(t_{j+1})) \right]. \end{aligned} \tag{17}$$

Now putting the above approximations into Eq. (16), we obtain the corrector formula for $S(t_{k+1})$, $k = 0, 1, ..., N - 1$,

$$S(t_{k+1}) \approx S(0) + \frac{\rho^{-\varrho} h^\varrho}{\Gamma(\varrho+2)} \sum_{j=0}^k a_{j,k+1} \mathcal{L}_1(t_j, S(t_j)) + \frac{\rho^{-\varrho} h^\varrho}{\Gamma(\varrho+2)} \mathcal{L}_1(t_{k+1}, S(t_{k+1})), \tag{18}$$

where

$$a_{j,k+1} = \begin{cases} k^{\varrho+1} - (k-\varrho)(k+1)^\varrho & \text{if } j = 0, \\ (k-j+2)^{\varrho+1} + (k-j)^{\varrho+1} - 2(k-j+1)^{\varrho+1} & \text{if } 1 \leq j \leq k. \end{cases} \tag{19}$$

In order to obtain the predictor value $S^P(t_{k+1})$, we apply the one-step Adams- Bashforth method to the integral equation (15). In this case, by replacing the function $\mathcal{L}_1(z^{1/\rho}, S(z^{1/\rho}))$ by the quantity $\mathcal{L}_1(t_j, S(t_j))$ at each integral in Eq. (16), we get

$$\begin{aligned} S^P(t_{k+1}) &\approx S(0) + \frac{\rho^{-\varrho}}{\Gamma(\varrho)} \sum_{j=0}^k \int_{t_j^\rho}^{t_{j+1}^\rho} (t_{k+1}^\rho - z)^{\varrho-1} \mathcal{L}_1(t_j, S(t_j)) dz \\ &= S(0) + \frac{\rho^{-\varrho} h^\varrho}{\Gamma(\varrho+1)} \sum_{j=0}^k [(k+1-j)^\varrho - (k-j)^\varrho] \mathcal{L}_1(t_j, S(t_j)). \end{aligned} \tag{20}$$

Now replacing $S(t_{k+1})$ given in the right side of (18) by $S^P(t_{k+1})$, our P-C algorithm, for finding the approximation $S_{k+1} \approx S(t_{k+1})$, is completely expressed by the formula

$$S_{k+1} \approx S(0) + \frac{\rho^{-\varrho}h^\varrho}{\Gamma(\varrho+2)} \sum_{j=0}^{k} a_{j,k+1}\mathcal{L}_1(t_j, S_j) + \frac{\rho^{-\varrho}h^\varrho}{\Gamma(\varrho+2)}\mathcal{L}_1(t_{k+1}, S^P_{k+1}), \qquad (21)$$

where $S_j \approx S(t_j)$, $j = 0, 1, ..., k$, and the predicted value $S^P_{k+1} \approx S^P(t_{k+1})$ is given in Eq. (20) with the weights $a_{j,k+1}$ being defined according to (19).

So, the Predictor-Corrector formulae for the system (7) are given by

$$S_{k+1} \approx S(0) + \frac{\rho^{-\varrho}h^\varrho}{\Gamma(\varrho+2)} \sum_{j=0}^{k} a_{j,k+1}\mathcal{L}_1(t_j, S_j) + \frac{\rho^{-\varrho}h^\varrho}{\Gamma(\varrho+2)}\mathcal{L}_1(t_{k+1}, S^P_{k+1}),$$

$$I_{k+1} \approx I(0) + \frac{\rho^{-\varrho}h^\varrho}{\Gamma(\varrho+2)} \sum_{j=0}^{k} a_{j,k+1}\mathcal{L}_2(t_j, I_j) + \frac{\rho^{-\varrho}h^\varrho}{\Gamma(\varrho+2)}\mathcal{L}_2(t_{k+1}, I^P_{k+1}),$$

$$R_{k+1} \approx R(0) + \frac{\rho^{-\varrho}h^\varrho}{\Gamma(\varrho+2)} \sum_{j=0}^{k} a_{j,k+1}\mathcal{L}_3(t_j, R_j) + \frac{\rho^{-\varrho}h^\varrho}{\Gamma(\varrho+2)}\mathcal{L}_3(t_{k+1}, R^P_{k+1}),$$

$$V_{k+1} \approx V(0) + \frac{\rho^{-\varrho}h^\varrho}{\Gamma(\varrho+2)} \sum_{j=0}^{k} a_{j,k+1}\mathcal{L}_4(t_j, V_j) + \frac{\rho^{-\varrho}h^\varrho}{\Gamma(\varrho+2)}\mathcal{L}_4(t_{k+1}, V^P_{k+1}),$$

$$(22)$$

where

$$S^P(t_{k+1}) \approx S(0) + \frac{\rho^{-\varrho}h^\varrho}{\Gamma(\varrho+1)} \sum_{j=0}^{k} [(k+1-j)^\varrho - (k-j)^\varrho]\mathcal{L}_1(t_j, S(t_j)),$$

$$I^P(t_{k+1}) \approx I(0) + \frac{\rho^{-\varrho}h^\varrho}{\Gamma(\varrho+1)} \sum_{j=0}^{k} [(k+1-j)^\varrho - (k-j)^\varrho]\mathcal{L}_2(t_j, I(t_j)),$$

$$R^P(t_{k+1}) \approx R(0) + \frac{\rho^{-\varrho}h^\varrho}{\Gamma(\varrho+1)} \sum_{j=0}^{k} [(k+1-j)^\varrho - (k-j)^\varrho]\mathcal{L}_3(t_j, R(t_j)),$$

$$V^P(t_{k+1}) \approx V(0) + \frac{\rho^{-\varrho}h^\varrho}{\Gamma(\varrho+1)} \sum_{j=0}^{k} [(k+1-j)^\varrho - (k-j)^\varrho]\mathcal{L}_4(t_j, V(t_j)).$$

$$(23)$$

Theorem 3 *[39] Assume that $\mathcal{L}_1(t, S)$, $\mathcal{L}_2(t, I)$, $\mathcal{L}_3(t, R)$, $\mathcal{L}_4(t, V)$ satisfy the Lipschitz condition and S_j, I_j, R_j, V_j ($j = 1, ..., k+1$) are the solutions of the Predictor-Corrector method* (22) *and* (23). *Then, the proposed numerical scheme is conditionally stable.*

Solution of the model by *Kumar-Erturk (K-E)* fractional numerical algorithm

Now we utilize one more method which is a very recent numerical method given by *Kumar et al.* in [42] to simulate nonlinear fractional-order IVPs. The scheme is defined by the following theorem:

Theorem 4 *Recall the IVP* (9a)-(9b). *Let*

$$\mathcal{F}(\nu, S_*(\nu)) = \mathcal{L}_1\left(\left\{ t^\rho - (t^\varrho - \nu\Gamma(\varrho+1)\rho^\varrho)^{\frac{1}{\varrho}} \right\}^{\frac{1}{\rho}}, S(t^\rho - (t^\varrho - \nu\Gamma(\varrho+1)\rho^\varrho)^{\frac{1}{\varrho}})^{\frac{1}{\rho}} \right),$$

with the assumption of Theorem 1 hold. Then, a solution of (9a)-(9b) *is defined by*

$$S(t) = S_*(t^\varrho\rho^{-\varrho}/\Gamma(\varrho+1)),$$

where $S_*(\nu)$ is a solution of classical differential equations

$$\frac{dS_*(\nu)}{d\nu} = \mathcal{F}(\nu, S_*(\nu)), \qquad (24)$$

and

$$S_*(0) = S_0. \qquad (25)$$

Proof Let us assume from Theorem 1 that $S(t)$ is a solution of (9a)-(9b) which also satisfies (10). Let $\tau^\rho = t^\rho - (t^\varrho - \nu\Gamma(\varrho+1)\rho^\varrho)^{1/\varrho}$. Then Eq. (10) can be re-written as

$$S(t) = S_0 + \int_0^{t^\varrho\rho^{-\varrho}/\Gamma(\varrho+1)} \mathcal{L}_1\left(\left\{t^\rho - (t^\varrho - \nu\Gamma(\varrho+1)\rho^\varrho)^{\frac{1}{\varrho}}\right\}^{\frac{1}{\rho}}, S(t^\rho - (t^\varrho - \nu\Gamma(\varrho+1)\rho^\varrho)^{\frac{1}{\varrho}})^{\frac{1}{\rho}}\right) d\nu \tag{26}$$

$$= S_0 + \int_0^{t^\varrho\rho^{-\varrho}/\Gamma(\varrho+1)} \mathcal{F}(\nu, S_*(\nu)) d\nu.$$

Also, every solution of (24)-(25) is the solution of the VIE given below and vice versa.

$$S_*(\nu) = S_0 + \int_0^\nu \mathcal{F}(s, S_*(s)) ds, \quad 0 \le \nu \le a^\varrho \rho^{-\varrho}/\Gamma(\varrho+1). \tag{27}$$

Since, $0 \le t^\varrho\rho^{-\varrho}/\Gamma(\varrho+1) \le a^\varrho\rho^{-\varrho}/\Gamma(\varrho+1)$, the right-hand side of equation (26) is equal to $S_*(t^\varrho\rho^{-\varrho}/\Gamma(\varrho+1))$. ∎

Now we derive the numerical solution of the considered model (7) based on the above methodology. Firstly, the corresponding classical model is

$$\frac{dS_*}{d\nu} = b - S_* - \beta S_* I_* + \nu V_* + \gamma R_*,$$

$$\frac{dI_*}{d\nu} = -dI_* + \beta S_* I_* - \sigma I_* - \omega I_* - \alpha I_*,$$

$$\frac{dR_*}{d\nu} = -dR_* + \alpha I_* - \gamma R_*,$$

$$\frac{dV_*}{d\nu} = \sigma I_* - \nu V_*. \tag{28}$$

If the solution of this system is $(S_*(\nu), I_*(\nu), R_*(\nu), V_*(\nu))$, then the solution of the model is $(S_*(t^\varrho/\Gamma(\varrho+1)), I_*(t^\varrho/\Gamma(\varrho+1)), R_*(t^\varrho/\Gamma(\varrho+1)), V_*(t^\varrho/\Gamma(\varrho+1)))$.

Remark 1 *This method is one of the fast numerical methods as compared to other available methods to solve the fractional-order initial value problems. The output processing time of the algorithm is very less, which means the scheme gives the outputs in a very short of time. Also, it is very easy to code this algorithm via any software like, Mathematica, Maple or MATLAB.*

6 Simulation results

Now we perform the analysis for the given cholera model (7) with the help of real parameter values given in Table 1. For the initial values of all four classes of cholera model, we assume $S(0) = 20000, I(0) = 30, R(0) = 0$ and $V(0) = 1000000$. In Figure 1, we plotted the graphs of infectious class $I(t)$ versus time variable t at various fractional order values along with the fixed values of extra parameter $\rho = 0.75$ by using both (K-E and P-C) numerical methods. Where-from sub-figure 1a we can observe the variations in the infected individuals by K-E method and from sub-figure 1b by using P-C method. We can see that the outputs of both methods are slightly different. In the case of K-E method, as much as time increasing, the infectious population is converging to the lower values much faster than the case of P-C method.

(a) Output via K-E method

(b) Output via modified P-C method
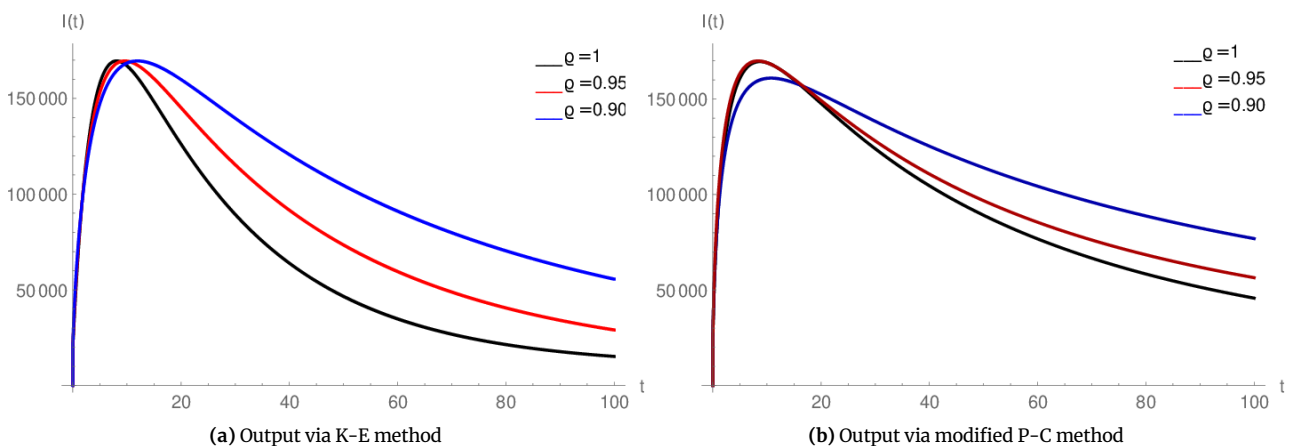
Figure 1. Dynamics of infectious class $I(t)$ at fractional-order values ϱ= 1, 0.95, 0.90.

(a) Output via K-E method

(b) Output via modified P-C method
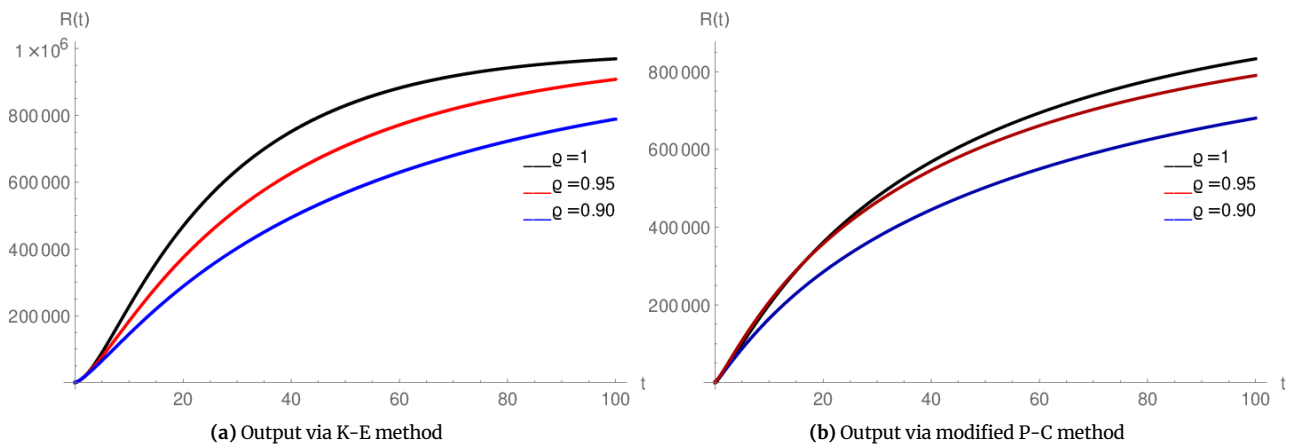
Figure 2. Dynamics of recovered class $R(t)$ at fractional-order values ϱ= 1, 0.95, 0.90.

(a) Output via K-E method

(b) Output via modified P-C method
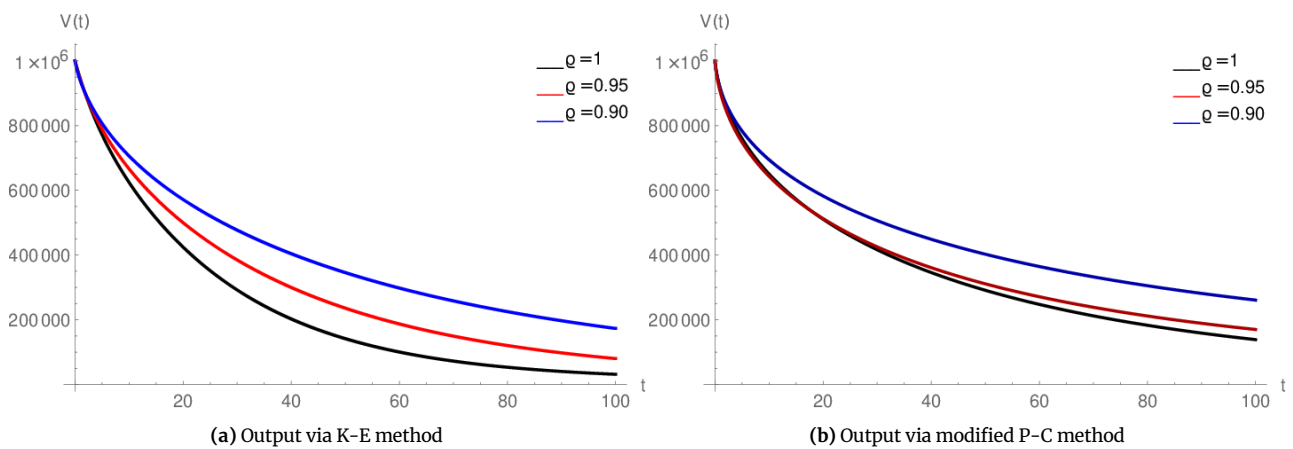
Figure 3. Dynamics of enviroment $V(t)$ at fractional-order values ϱ= 1, 0.95, 0.90.

In Figure 2, the graphs of recovered class $R(t)$ versus time variable t at various fractional orders along with ρ = 0.75 by using both numerical methods are given. From sub-figure 2a, we can see the variations in the recovered individuals by K-E method and from sub-figure 2b by using P-C method. Again the outputs of both methods are slightly different. In the case of K-E method, the recovered population is increasing much faster then the case of P-C method. Similarly, decrement in the environmental infection or the number of bacteria concentrations $V(t)$ can be observed from Figure 3 (sub-figure 3a via K-E method and sub-figure 3b via P-C method). For understanding the role of extra parameter ρ, we plotted the group of Figures 4, 5, and 6. Here we notice that the variations caused by extra parameter ρ in K-E method (sub-figures 4a, 5a, 6a) are totally reverse to the variations caused by ρ in P-C method (sub-figures 4b, 5b, 6b). It means that both methods process the role of ρ in a different way, which makes their comparison more interesting.

(a) Output via K-E method

(b) Output via modified P-C method
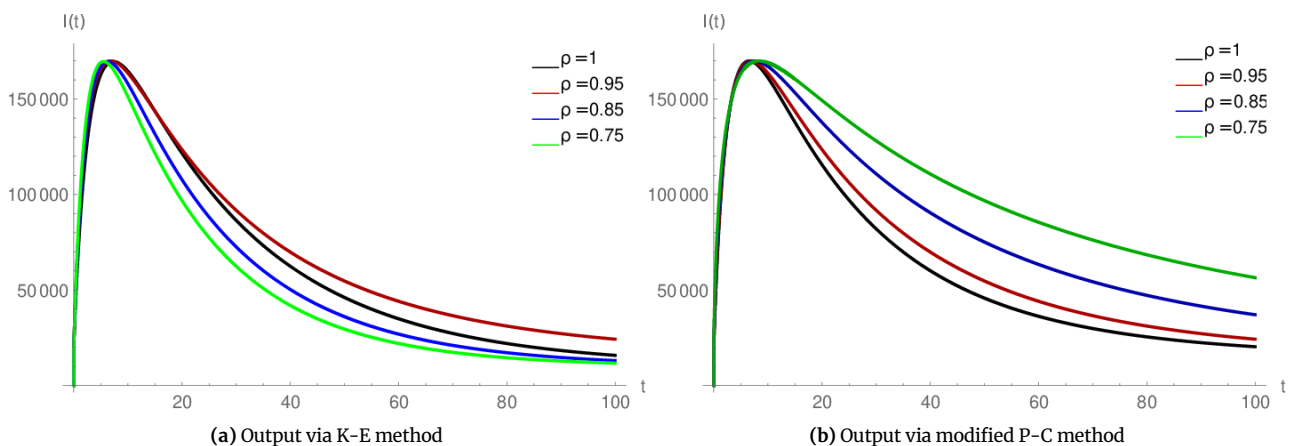
Figure 4. Variations caused by extra parameter ρ in class $I(t)$ at fractional-order ϱ= 0.95.
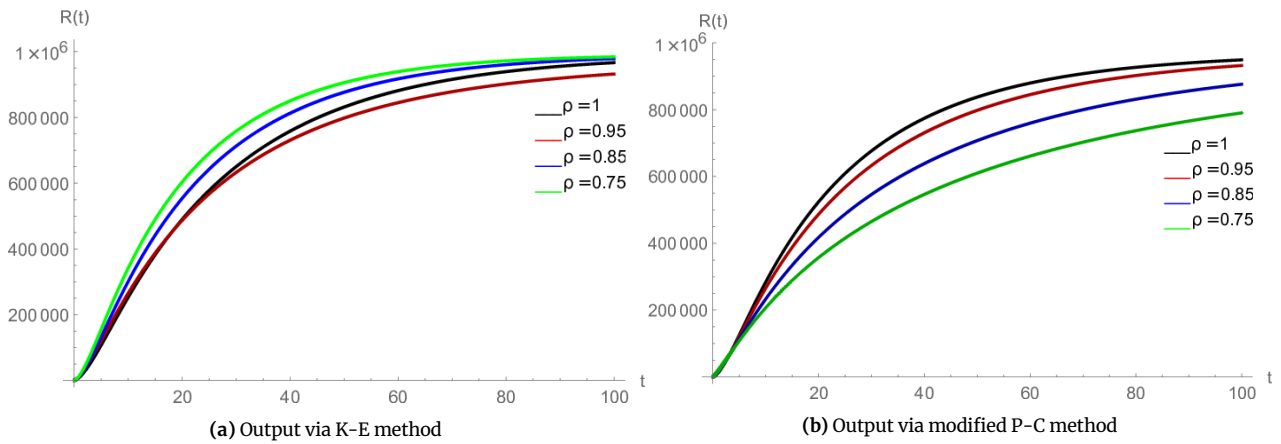
Figure 5. Variations caused by extra parameter ρ in class $R(t)$ at fractional-order $\varrho = 0.95$.
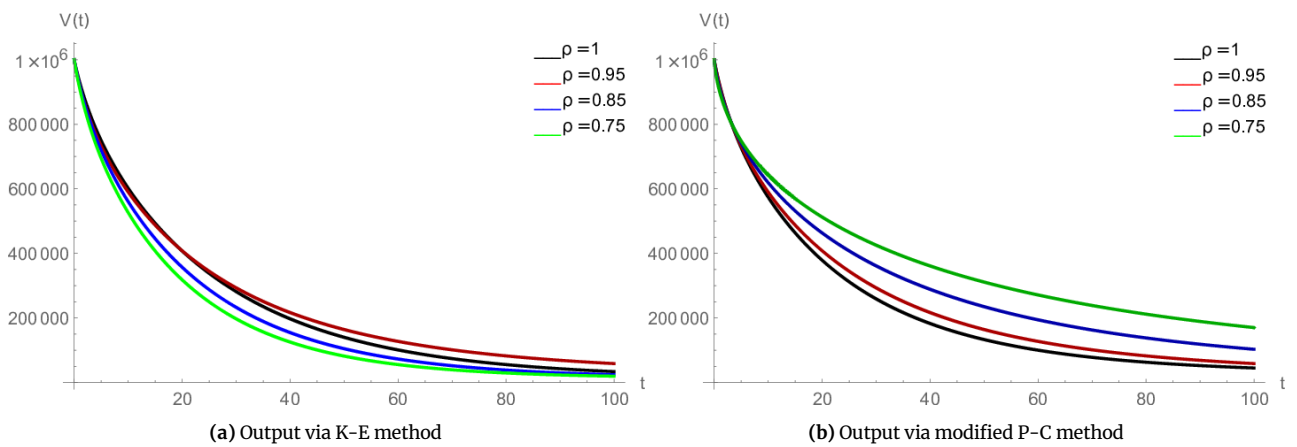
Figure 6. Variations caused by extra parameter ρ in class $V(t)$ at fractional-order $\varrho = 0.95$.

From the above given graphical simulations, we can see that both methods perform well to simulate the dynamics of the given cholera model. The outputs of both methods are slightly different which justify the importance of both schemes in this study. But when we compare the processing speed of both methods then K-E method is very fast as compared to P-C scheme because it takes only $1/4th$ processing time of the P-C method. The stability of the given P-C method is available as mentioned in Theorem 3 but the analysis related to the stability of K-E method still needs to be studied.

7 Conclusion

In this research work, we have investigated a mathematical model of cholera disease in the sense of the generalised Liouville-Caputo fractional derivative. We have proved the results for the existence of a unique solution. Numerical solutions to the considered model have been derived with the help of two different methods and the importance of both schemes has been justified. A couple of figures are simulated to explore the given cholera disease dynamics. The main aim of this work has been to explore the given disease dynamics as well as the efficiency, accuracy, and differences of both numerical methods. In the future, the given model can be solved by using any other fractional derivatives and the proposed schemes can be utilized to solve different types of non-linear fractional order models.

Declarations

Consent for publication

Not applicable.

Data availability statement

The data used in this study are mentioned/available in the manuscript.

Conflicts of interest

The authors declare that they have no conflict of interests.

Funding

Author's contributions

P.K.: Conceptualization, Investigation, Formal analysis, Resources, Visualization, Writing - original draft. V.S.E.: Investigation, Software, Writing-Reviewing and Editing. All authors discussed the results and contributed to the final manuscript.

Acknowledgements

References

[1] Piarroux, R., Barrais, R., Faucher, B., Haus, R., Piarroux, M., Gaudart, J., Magloire, R. & Raoult, D. Understanding the cholera epidemic, Haiti. *Emerging infectious diseases*, 17(7), 1161, (2011). [CrossRef]

[2] Tappero, J.W. & Tauxe, R.V. Lessons learned during public health response to cholera epidemic in Haiti and the Dominican Republic. *Emerging infectious diseases*, 17(11), 2087,(2011). [CrossRef]

[3] Lemos-Paião, A.P., Silva, C.J. & Torres, D.F. An epidemic model for cholera with optimal control treatment. *Journal of Computational and Applied Mathematics*, 318, 168-180, (2017). [CrossRef]

[4] Eustace, K.A., Osman, S. & Wainaina, M. Mathematical modelling and analysis of the dynamics of cholera. *Global Journal of Pure and Applied Mathematics*, 14(9), 1259-1275, (2018). [CrossRef]

[5] Sun, G.Q., Xie, J.H., Huang, S.H., Jin, Z., Li, M.T. & Liu, L. Transmission dynamics of cholera: Mathematical modeling and control strategies. *Communications in Nonlinear Science and Numerical Simulation*, 45, 235-244, (2017). [CrossRef]

[6] Njagarah, J.B.H. & Tabi, C.B. Spatial synchrony in fractional order metapopulation cholera transmission. *Chaos, Solitons & Fractals*, 117, 37-49, (2018). [CrossRef]

[7] Kilbas, A., Srivastava, H.M., and Trujillo, J.J. *Theory and Applications of Fractional Differential Equations*. Elsevier Science, (2006).

[8] Podlubny, I. *Fractional Differential Equations: An Introduction to Fractional Derivatives, Fractional Differential Equations, to Methods of their Solution and Some of their Applications*. Elsevier, (1998).

[9] Kumar, P. & Erturk, V.S. The analysis of a time delay fractional COVID-19 model via Caputo type fractional derivative. *Mathematical Methods in the Applied Sciences*, (2020). [CrossRef]

[10] Kumar, P., Erturk, V.S., Abboubakar, H. & Nisar, K.S. Prediction studies of the epidemic peak of coronavirus disease in Brazil via new generalised Caputo type fractional derivatives. *Alexandria Engineering Journal*, 60(3), 3189-3204, (2021). [CrossRef]

[11] Gao, W., Veeresha, P., Baskonus, H.M., Prakasha, D.G. & Kumar, P. A New Study of Unreported Cases of 2019-nCOV Epidemic Outbreaks. *Chaos, Solitons & Fractals*,138, 109929, (2020). [CrossRef]

[12] Nabi, K.N., Abboubakar, H. & Kumar, P. Forecasting of COVID-19 pandemic: From integer derivatives to fractional derivatives. *Chaos, Solitons & Fractals*, 141, 110283, (2020). [CrossRef]

[13] Nabi, K.N., Kumar, P. & Erturk, V.S. Projections and fractional dynamics of COVID-19 with optimal control strategies. *Chaos, Solitons & Fractals*, 145, 110689, (2021). [CrossRef]

[14] Kumar, P., Erturk, V.S., & Murillo-Arcila, M. A new fractional mathematical modelling of COVID-19 with the availability of vaccine.*Results in Physics*, 24, 104213, (2021). [CrossRef]

[15] Naik, P.A., Yavuz, M., Qureshi, S., Zu, J. & Townley, S. Modeling and analysis of COVID-19 epidemics with treatment in fractional derivatives using real data from Pakistan. *The European Physical Journal Plus*, 135(10), 1-42, (2020). [CrossRef]

[16] Özköse, F., & Yavuz, M. Investigation of interactions between COVID-19 and diabetes with hereditary traits using real data: A case study in Turkey. *Computers in biology and medicine,* 105044, (2022). [CrossRef]

[17] Ikram, R., Khan, A., Zahri, M., Saeed, A., Yavuz, M. & Kumam, P. Extinction and stationary distribution of a stochastic COVID-19 epidemic model with time-delay. *Computers in Biology and Medicine*, 141, 105115, (2022). [CrossRef]

[18] Allegretti, S., Bulai, I.M., Marino, R., Menandro, M.A. & Parisi, K. Vaccination effect conjoint to fraction of avoided contacts for a Sars-Cov-2 mathematical model. *Mathematical Modelling and Numerical Simulation with Applications (MMNSA)*, 1(2), 56-66, (2021). [CrossRef]

[19] Kumar, P., Erturk, V.S., Yusuf, A. & Kumar, S. Fractional time-delay mathematical modeling of Oncolytic Virotherapy. *Chaos, Solitons & Fractals*, 150, 111123, (2021). [CrossRef]

[20] Abboubakar, H., Kumar, P., Erturk, V.S. & Kumar, A. A mathematical study of a Tuberculosis model with fractional derivatives. *International Journal of Modeling, Simulation, and Scientific Computing*, 2150037, (2021). [CrossRef]

[21] Abboubakar, H., Kumar, P., Rangaig, N.A. & Kumar, S. A Malaria Model with Caputo-Fabrizio and Atangana-Baleanu Derivatives. *International Journal of Modeling, Simulation, and Scientific Computing*, 12(02), 2150013, (2020). [CrossRef]

[22] Kumar, P., Erturk, V.S., Yusuf, A. & Sulaiman, T.A. Lassa hemorrhagic fever model using new generalized Caputo-type fractional derivative operator. *International Journal of Modeling, Simulation, and Scientific Computing*, 12(06), 2150055, (2021). [CrossRef]

[23] Kumar, P., Erturk, V.S., Yusuf, A., Nisar, K.S. & Abdelwahab, S.F. A study on canine distemper virus (CDV) and rabies epidemics in the red fox population via fractional derivatives. *Results in Physics*, 25, 104281, (2021). [CrossRef]

[24] Kumar, P., Erturk, V.S. & Murillo-Arcila, M. A complex fractional mathematical modeling for the love story of Layla and Majnun. *Chaos, Solitons & Fractals*, 150, 111091, (2021). [CrossRef]

[25] Kumar, P. & Erturk, V.S. Environmental persistence influences infection dynamics for a butterfly pathogen via new generalised Caputo type fractional derivative. *Chaos, Solitons & Fractals*, 144, 110672, (2021). [CrossRef]

[26] Kumar, P., Erturk, V.S., Banerjee, R., Yavuz, M. & Govindaraj, V. Fractional modeling of plankton-oxygen dynamics under climate change by the application of a recent numerical algorithm. *Physica Scripta*, 96(12), 124044, (2021). [CrossRef]

[27] Kumar, P., Erturk, V.S. & Nisar, K.S. Fractional dynamics of huanglongbing transmission within a citrus tree. *Mathematical Methods in the Applied Sciences*, (2021). [CrossRef]

[28] Kumar, P., Erturk, V.S. & Almusawa, H. Mathematical structure of mosaic disease using microbial biostimulants via Caputo and Atangana−Baleanu derivatives. *Results in Physics*, 24, 104186, (2021). [CrossRef]

[29] Joshi, H. & Jha, B.K. Fractional-order mathematical model for calcium distribution in nerve cells. *Computational and Applied Mathematics*, 39(2), 1-22, (2020). [CrossRef]

[30] Joshi, H. & Jha, B.K. On a reaction−diffusion model for calcium dynamics in neurons with Mittag−Leffler memory. *The European Physical Journal Plus*, 136(6), 1-15, (2021). [CrossRef]

[31] Joshi, H. & Jha, B.K. Chaos of calcium diffusion in Parkinson's infectious disease model and treatment mechanism via Hilfer fractional derivative. *Mathematical Modelling and Numerical Simulation with Applications (MMNSA)*, 1(2), 84-94, (2021). [CrossRef]

[32] Joshi, H. & Jha, B.K. Modeling the spatiotemporal intracellular calcium dynamics in nerve cell with strong memory effects. *International Journal of Nonlinear Sciences and Numerical Simulation*, (2021). [CrossRef]

[33] Veeresha, P. A numerical approach to the coupled atmospheric ocean model using a fractional operator. *Mathematical Modelling and Numerical Simulation with Applications (MMNSA)*, 1(1), 1-10, (2021). [CrossRef]

[34] Baishya, C. & Veeresha, P. Laguerre polynomial-based operational matrix of integration for solving fractional differential equations with non-singular kernel. *Proceedings of the Royal Society A*, 477(2253), 20210438, (2021). [CrossRef]

[35] Veeresha, P. & Baleanu, D. A unifying computational framework for fractional Gross−Pitaevskii equations. *Physica Scripta*, 96(12), 125010, (2021). [CrossRef]

[36] Akinyemi, L., Nisar, K.S., Saleel, C.A., Rezazadeh, H., Veeresha, P., Khater, M.M. & Inc, M. Novel approach to the analysis of fifth-order weakly nonlocal fractional Schrödinger equation with Caputo derivative. *Results in Physics*, 31, 104958, (2021). [CrossRef]

[37] Okposo, N.I., Veeresha, P. & Okposo, E.N. Solutions for time-fractional coupled nonlinear Schrödinger equations arising in optical solitons. *Chinese Journal of Physics*, (2021). [CrossRef]

[38] Odibat, Z. and Baleanu, D. Numerical simulation of initial value problems with generalized caputo-type fractional derivatives. *Applied Numerical Mathematics*, 156, 94-105, (2020). [CrossRef]

[39] Erturk, V.S. & Kumar, P. Solution of a COVID-19 model via new generalized Caputo-type fractional derivatives. *Chaos, Solitons & Fractals*, 139, 110280, (2020). [CrossRef]

[40] Kumar, P. & Erturk, V.S. A case study of Covid-19 epidemic in India via new generalised Caputo type fractional derivatives. *Mathematical Methods in the Applied Sciences*, 1-14, (2021). [CrossRef]

[41] Odibat, Z., Erturk, V.S., Kumar, P. & Govindaraj, V. Dynamics of generalized Caputo type delay fractional differential equations using a modified Predictor-Corrector scheme. *Physica Scripta*, 96(12), 125213, (2021). [CrossRef]

[42] Kumar, P., Erturk, V.S. & Kumar, A. A new technique to solve generalized Caputo type fractional differential equations with the example of computer virus model. *Journal of Mathematical Extension*, 15, (2021). [CrossRef]

Mathematical Modelling and Numerical Simulation with Applications (MMNSA) (http://www.mmnsa.org)